Fiber Fuse Phenomenon in Step-Index Single-Mode Optical Fibers

Yoshito Shuto, *Member, IEEE*, Shuichi Yanagi, Shuichiro Asakawa, *Member, IEEE*, Masaru Kobayashi, *Member, IEEE*, and Ryo Nagase, *Member, IEEE*

***Abstract*—The unsteady-state thermal conduction process in step-index single-mode (SM) optical fiber was studied theoretically with the explicit finite-difference method. We considered a high-temperature loss-increase mechanism, which includes two factors that bring about an increase in the absorption coefficients: 1) electronic conductivity due to the thermal ionization of a Ge-doped silica core and 2) thermochemical SiO production in silica glass. The core-center temperature changed suddenly and reached over 4×10^5 K when a 1.064-μm laser power of 2 W was input into the core layer heated at 2723 K. This rapid heating of the core initiated the "fiber fuse" phenomenon. The high-temperature core areas were enlarged and propagated toward the light source. The propagation rates of the fiber fuse, estimated at 1.064 and 1.48 μm, were in fair agreement with the experimentally determined values. We found that the threshold power for initiating the fiber fuse increases from 0.98 to 1.26 W when the input laser wavelength is increased from 1.06 to 1.55 μm.**

***Index Terms*—Absorption coefficient, electrical conductivity, fiber fuse phenomenon, point defect, single-mode (SM) optical fiber, thermal conduction.**

I. Introduction

BROAD-BAND Raman amplifiers pumped by high-power laser diodes have been developed for wavelength-division-multiplexed (WDM) transmission systems [1]–[4]. In Raman amplifiers, optical signals can be amplified in an optical fiber through a power transfer from the pump to the signal via the stimulated Raman scattering process. For optical signals at 1.525–1.615 μm (C- and L-band), the Raman amplifiers are pumped at 1.420–1.510 μm [4]. To obtain a large Raman gain, Raman amplifier-based optical network systems require high-power pump sources that operate at 1.420–1.510 μm. For this purpose, 1.4XX-μm pump laser diodes have achieved more than 300 mW at a commercial level, and several W-class 1.480-μm Raman lasers are commercially available. In optical network systems, there is a possibility that high-power optical signals will be transmitted through single-mode (SM) optical fibers. As the optical power level rises, nonlinear phenomena start to become important, and these include the effects of the "fiber fuse'" phenomenon. This effect, named because of its similarity in appearance to a burning fuse, can lead to the catastrophic destruction of various types of optical fiber [5].

The fiber fuse phenomenon was first observed in 1987 by Kashyap and Blow [6], [7]. Most experimental results focused on an intensity level of $1 \sim 3$ MW/cm^2. This is many orders of magnitude below the intrinsic damage limit for silica of > 10 GW/cm^2 [6]. The fiber fuse typically involves a zone of absorption that melts and then vaporizes the core at several thousand kelvin, creating a void. The creation of this void is followed by the initiation of another void further down the core in the direction of the optical power source. This process is rapidly repeated, moving an intense blue-white flash down the fiber at velocities of the order of 1 m/s [6]–[14]. Fig. 1 shows damage centers in the core of a damaged fiber. The damage is made manifest by the periodic bullet-shaped cavities left in the core. These cavities were considered to be the result of a classic Rayleigh instability caused by capillary effects in the molten silica that surrounds a vaporized fiber core [15]. Fuses are terminated by gradually reducing the laser power to provide a termination threshold at which the speed of the fuse is reduced to zero.

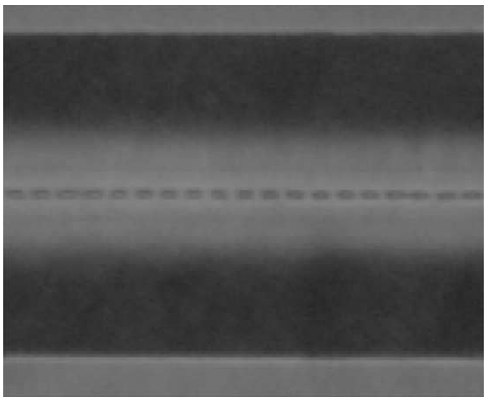

Fig. 1. Damage centers in the core of a damaged fiber.

Several hypotheses have been put forward to explain the fiber fuse phenomenon. These include a chemical reaction involving the exothermal formation of germanium defects [8], self-propelled self-focusing [6], and thermal lensing of the light in the fiber via a solitary thermal shock wave [9]. In experiments, this phenomenon can be initiated by bringing the fiber output end into contact with absorbent materials [6] and/or heating the fiber with a flame or arc discharge [7]–[14].

The light absorption coefficient α of the fiber core at high temperatures is closely related to the generation of the fiber fuse phenomenon. Kashyap reported that there was a rapid increase in the α value of a germanium (Ge)-doped silica core above the critical temperature T_0 ($\sim$ 1323 K), while the α value of about 0 dB/km at room temperature remained unchanged until the temperature (T) approached T_0 [7]. The α value increased by nearly 1900 dB/km (~ 0.44 m^{-1}) at 1.064 μm when T

Manuscript received February 11, 2004; revised April 16, 2004.

The authors are with NTT Photonics Laboratories, Nippon Telegraph and Telephone Corporation, Atsugi, Japan (e-mail: shuto@aecl.ntt.co.jp).

Digital Object Identifier 10.1109/JQE.2004.831635

changed from T_0 to T_0+50 K. Hand and Russell found that this phenomenon was initiated by the generation of large numbers of Ge-related defects at high temperatures above about 1273 K, and the α values at 0.5 μm induced at temperatures below 1873 K were modeled quite accurately using an Arrhenius equation [9], [10].

By contrast, they reported that the best fit between the experimental and theoretical fiber fuse velocities was obtained when the α value of the Ge-doped silica core at 2293 K was assumed to be 5.6×10^4 m^{-1} at 0.5 μm [9]. This large α value, however, could not be estimated by using their Arrhenius equation [9], [10]. Therefore, the exact mechanism causing the increases in the optical absorption in a Ge-doped silica core at high temperatures remained unclear until now.

Furthermore, Hand and Russell reported that the electrical conductivity σ of the fiber core increased with temperature and the hot spot at the fuse center was plasmalike [9]. Kashyap considered that the large α values may be attributable to an enlargement in the σ value of the fiber core at high temperatures above T_0 [7]. However, it is well known that silica glass is a good insulator at room temperature, and the electrical conductivity in silica glass below 1073 K is due to positively charged alkali ions moving under the influence of an applied field [16], [17]. The ionic conduction in the glass is not related solely to the optical absorption. Therefore, the exact mechanism causing the increase in the σ value and the relationship between σ and α in silica glass at high temperatures above 1273 K has also remained unclear until now.

In this paper, we describe a high-temperature loss-increase mechanism in the SM optical fibers and estimate high-temperature α values at laser wavelengths of >1 μm. We use these values to study the unsteady-state thermal conduction process in a step-index SM optical fiber theoretically with the explicit finite-difference technique.

II. High-Temperature Optical Absorption in Optical Fibers

A. Point Defect Formation and Electronic Conduction

It is well known that point (Frenkel) defects (Si E' and Ge E' centers) are induced in Ge-doped silica-core optical fiber at high temperatures [18], [19]. E' centers are associated with oxygen vacancies $\equiv$ X $-$ Si $\equiv$ (X = Ge or Si) [20]. Ge E' centers are stable at high temperatures above 873 K, but the Si E' center concentration decreases above 573 K and cannot be measured above 973 K [19]. In their fiber fuse experiments, Hand and Russell found that ESR studies of damaged Ge-doped silica-core fiber showed a strong Ge E' fingerprint [9]. Therefore, the Ge E' centers play an important role in the fiber fuse phenomenon.

The thermally induced Ge E' centers are produced through the following reactions:

$$\equiv \mathrm{Ge}-\mathrm{O}-\mathrm{Si}\equiv \;\rightarrow \equiv \mathrm{Ge}-\mathrm{Si}\equiv + \left(\frac{1}{2}\right)\mathrm{O}_2\uparrow \quad (1)$$

$$\equiv \mathrm{Ge}-\mathrm{Si}\equiv \;\rightarrow \equiv \mathrm{Ge}^{\bullet}\mathrm{Si}^{+}\equiv + e^{-}. \quad (2)$$

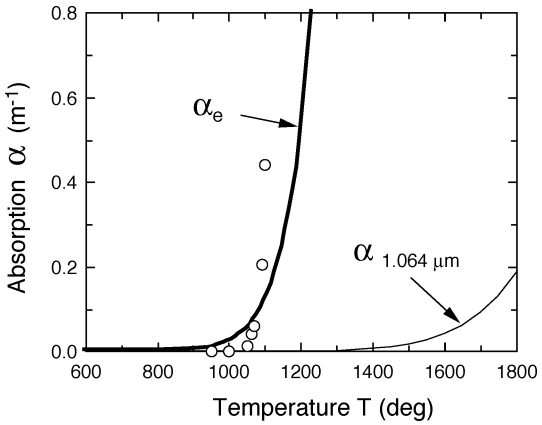

Fig. 2. Temperature dependence of absorption induced by heating Ge (4 mol%)-doped silica-core fibers. The thin and thick solid lines were calculated by using (6) and (4), respectively. The open circles are the data reported by Kashyap [7].

According to the point defect model [19], the Ge E' concentration $n_{\mathrm{Ge}E'}$ in the Ge (4 mol %)-doped silica-core fiber heated at T is obtained as

$$n_{\mathrm{Ge}E'} = n_p \exp\left(-\frac{E_f}{kT}\right) \quad (3)$$

where E_f $(=2.5$ eV) is the formation energy of the Ge E' centers, n_p $(=1.72\times10^{21}$ cm$^{-3})$ is the concentration of the precursors of the Ge E' centers, and k is Boltzmann's constant.

Equation (2) represents the thermal ionization of the Si atoms in the precursor $\equiv$ Ge $-$ Si $\equiv$, together with the formation of the Ge E' centers. The electrons produced in this process can move in the silica core. This means that the thermally ionized silica core has a measurable electrical conductivity σ. As the electron concentration $n_e = n_{\mathrm{Ge}E'}$, the temperature dependence of σ for a Ge (4 mol %)-doped silica core is approximately given by

$$\sigma = e\mu_e n_e \sim e\mu_e n_p \exp\left(-\frac{E_f}{kT}\right) \quad (4)$$

where e is the electronic charge, and μ_e is the drift mobility of electrons in the silica core. The μ_e value obtained from the measurements ranged from 7 to 63 cm^2/V s [21] because the intrinsic drift mobility was masked by electron trapping or impurity scattering, which always give μ_e values that are lower than the intrinsic value.

The absorption α_e due to the σ value is given by [22]

$$\alpha_e \sim \frac{c_0\mu_0\sigma}{2n_1} \quad (5)$$

where μ_0 and c_0 are the permeability and the velocity of light in a vacuum, respectively. n_1 (~ 1.46) is the refractive index of the core.

By using $\mu_e = 50$ cm^2/V s and (4) and (5), we can estimate the α_e values as a function of T. The result is shown as a thick solid line in Fig. 2. The data reported by Kashyap (measured at 1.064 μm) [7] are plotted in this figure. The calculated α_e values appear to be in fairly good agreement with the experimental α values obtained at 1.064 μm.

It is noteworthy that the loss increase observed at 1.064 μm is not directly related to the absorption of the Ge E' centers.

It was found that the radiation-induced absorption coefficient α increased with the Ge E' center concentration [23], [24]. An α value of about 0.0594 m^{-1} was observed at 1.064 μm for $n_{GeE'} = 1.1 \times 10^{15}$ cm^{-3} [23]. By using (3), the α value, which is related to the Ge E' center, of the Ge (4 mol %)-doped silica-core fiber measured at 1.064 μm is given by

$$\alpha_{1.064\ \mu\mathrm{m}} = \alpha^0_{1.064\ \mu\mathrm{m}} \exp\left(-\frac{E_f}{kT}\right) \tag{6}$$

where $\alpha^0_{1.064\ \mu\mathrm{m}} = 9.29 \times 10^4$ m^{-1}. By using (6), the α values at 1.064 μm can be calculated as a function of T. The results are shown as a thin solid line in Fig. 2. The calculated α values at 1.064 μm were much smaller than the experimental values. This means that the loss increase observed at 1.064 μm can be well explained by the electronic conductivity caused by the thermal ionization of a Ge-doped silica core, but it is not directly related to the absorption of the Ge E' centers.

It has been reported that large α values of the order of 10^4 m^{-1} are necessary to obtain the best fit between the experimental and theoretical fiber fuse velocities in Ge-doped silica-core fibers operating at high temperatures above 2273 K [7], [9]. We estimated the α_e values above 2273 K using $\mu_e = 50$ cm^2/V s and (4) and (5). The calculated α_e was 6.1×10^2 m^{-1} at 2873 K. This value was about two orders smaller than the α value ($1.0 - 4.0 \times 10^4$ m^{-1}) reported by Kashyap *et al.* [7], [13]. Furthermore, it has been reported that the μ_e values at high temperatures are gradually reduced by electron scattering via interaction with the longitudinal optical (LO) phonon modes [25]. Therefore, we need another loss-increase mechanism at high temperatures above 2273 K to explain the large (10^4 m^{-1}) α values.

B. Effect of SiO Formation on Absorption

It has been reported that, at elevated temperatures, silica glass is thermally decomposed by the reaction [26]

$$SiO_2 \rightleftarrows SiO + \left(\frac{1}{2}\right) O_2. \tag{7}$$

SiO vapor is condensable, and the color of SiO solid, which is produced by the slow quenching of SiO vapor, can range from light brown to black [27]. This color is similar to that of the slightly darkened material in the region immediately surrounding the fiber core damaged by the fiber fuse phenomenon [6]. If the thermodynamic equilibrium constant for (7) is K, the SiO concentration c_{SiO} is approximately given by the following equation under the neutral condition ($c_{SiO} = 2\, c_{O_2}$):

$$c_{SiO} \sim \sqrt[3]{2\left(c^0_{SiO_2} K\right)^2} - \left(\frac{2}{3}\right)\sqrt[3]{4c^0_{SiO_2} K^4} + \frac{2K^2}{3} \tag{8}$$

where $c^0_{SiO_2}$ ($\sim$ 0.037 mol cm^{-3}) is the initial concentration of SiO_2. The equilibrium constant K can be estimated by using the free energy change ΔF^0 for the corresponding reaction as follows:

$$\ln K = -\frac{\Delta F^0}{RT} = -\frac{\Delta H^0}{RT} + \frac{\Delta S^0}{R} \tag{9}$$

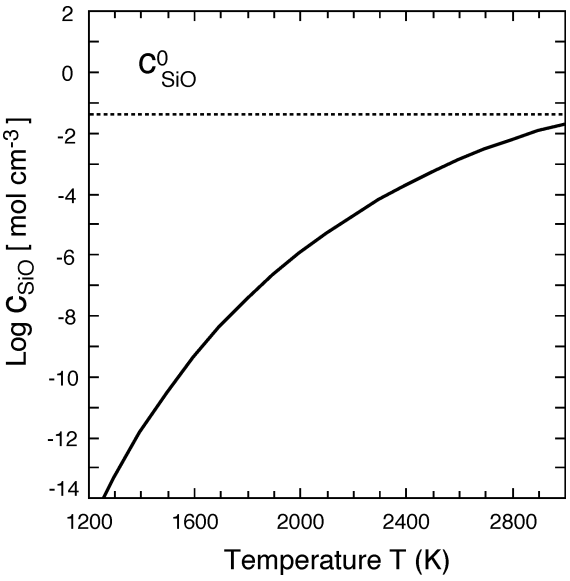

Fig. 3. Temperature dependence of the SiO concentration.

where R is the gas constant, and ΔH^0 and ΔS^0 are the heat of the reaction and the entropy change, respectively. The ΔF^0 values were estimated by using published thermochemical data [28] for SiO, O_2, and SiO_2. c_{SiO} can be calculated by using the estimated ΔF^0 values. The relationship between c_{SiO} and T is shown in Fig. 3. c_{SiO} increases with increasing T and gradually approaches its maximum value ($c^0_{SiO} \sim 0.048$ mol cm^{-3}) at $T >\sim 3000$ K.

Philipp reported that the optical absorption spectrum of SiO solid is similar to that of crystalline Si because there are many Si–Si bonds in SiO solid and that the absorption coefficients α_{SiO} for SiO near the threshold energy should be about one-twentieth the absorption α_{Si} for silicon [29]. The reducing factor (about one-twentieth) of the α value corresponded to the theoretical concentration of Si–(Si_4) tetrahedra in the SiO solid, which was estimated with the random bonding model [30]. In our calculation, however, we used one-thirtieth as the α value reducing factor. This reducing factor (one-thirtieth) was determined based on the fact that the homogeneity of the thermally produced SiO solid in the silica glass was very poor, compared with the SiO film prepared by Philipp.

The intrinsic α_{Si} values of crystalline Si were measured by Dash and Newman [31]. At photon energies E below 2.5 eV, the absorption edge spectrum of Si can be interpreted in terms of indirect optical transitions involving phonons [32]. The temperature dependence of the α_{Si} at $E < 2.5$ eV can be approximately described by the following equation [33]:

$$\alpha_{Si} = A_c \left[\frac{(E - E_g - k\theta)^2}{1 - e^{-\frac{\theta}{T}}} + \frac{(E - E_g + k\theta)^2}{e^{\frac{\theta}{T}} - 1}\right] \tag{10}$$

where E_g ($\sim$ 1.1 eV) is the energy gap, which varies with temperature, and $A_c \sim 4.47 \times 10^3 cm^{-1}eV^{-2}$. $\theta = 600$ K and $k\theta$ represents the phonon energy. It is well known that the E_g value decreases linearly with T at $T > 200$ K [32], [33]. Therefore, the E_g value (eV unit) at $T > 300$ K is given by

$$E_g = 1.110 - C_g(T - 300) \tag{11}$$

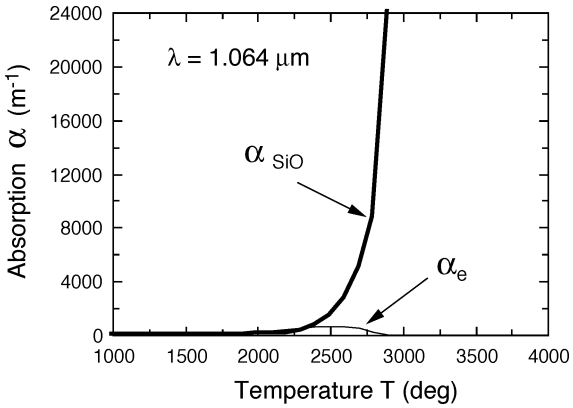

Fig. 4. Temperature dependence of the absorption at 1.064 μm induced by heating Ge (4 mol %)-doped silica-core fibers. The thin and thick solid lines were calculated by using (5) and (10), respectively.

where C_g (~ 1.4 to 2.6×10^{-4} eV/K) is the temperature coefficient of the energy gap. The $\alpha_{\rm SiO}$ values resulting from the SiO absorption at T can be estimated to be $\gamma\alpha_{\rm Si}(T)$, where $\gamma \equiv c_{\rm SiO}(T)/30c^0_{\rm SiO}$.

Therefore, the α values of Ge-doped silica-core fibers at high temperatures can be summarized as follows:

$$\alpha = \alpha_e + \alpha_{\rm SiO} \sim \frac{c_0\mu_0 e\mu_e n_p}{2n_1}\exp\left(\frac{-E_f}{kT}\right) + \frac{c_{\rm SiO}}{30c^0_{\rm SiO}}\alpha_{\rm Si}. \quad (12)$$

By using (5) and (10) and the calculated values shown in Fig. 3, we can calculate the temperature dependences of the α_e and $\alpha_{\rm SiO}$ values at 1.064 μm ($E = 1.17$ eV). The results are shown as two solid lines in Fig. 4. At 3123 K the $\alpha_{\rm SiO}$ value was about 2.0×10^4 m^{-1}. This α value is close to the experimental value ($1.0 - 4.0 \times 10^4$ m^{-1}) reported by Kashyap *et al.* [7], [13]. This means that the α value at high temperatures above 2273 K is mainly determined by the interband absorption of SiO thermochemically produced in the silica glass.

In Section III, we describe the results of some numerical calculations related to the thermal conduction process in a step-index SM optical fiber.

III. Simulation of Fiber Fuse in SM Optical Fiber

A. Heat Conduction in Optical Fiber

We assume the SM optical fiber to have a radius of r_f and to be in an atmosphere of $T = T_a$. We also assume that part of the core layer is heated and has a length of ΔL and a temperature of $T^0_c (> T_a)$ (see Fig. 5). In the hot zone, the α values are larger than those of the other parts of the core layer. Thus, as the light propagates along the normal direction (the direction away from the light source) in this zone, considerable heat is produced by light absorption.

The heat conduction equation for the temperature field $T(r, z, t)$ in step-index SM optical fiber is given by [34]

$$\rho C_p \frac{\partial T}{\partial t} = \kappa\left(\frac{\partial^2 T}{\partial r^2} + \frac{1}{r}\frac{\partial T}{\partial r} + \frac{\partial^2 T}{\partial z^2}\right) + \dot{Q} \quad (13)$$

where ρ, C_p, and κ are the density, the specific heat, and the thermal conductivity of the fiber, respectively. The last term $\dot{Q}$ in (13) represents the heat source caused by light absorption, which is required only for the hot zone in the fiber core. $\dot{Q}$ can be given by

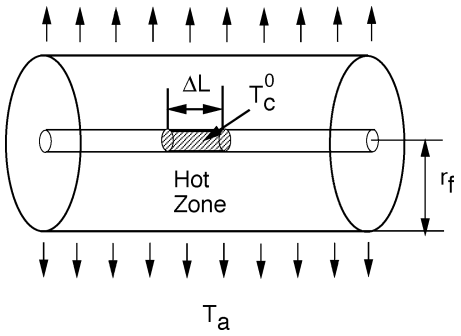

Fig. 5. Schematic view of the hot zone in the core layer.

$$\dot{Q} = \alpha I \quad (14)$$

where I is the optical power intensity of the core layer. We assume that the I value for the fundamental $\rm HE_{11}$ mode of step-index optical fiber can be given by dividing the transmission power in the core layer by the area of the spot size. That is, I is given by

$$I = \frac{P}{\pi r_s^2}\frac{w^2}{v^2}\left[1 + \frac{J_0^2(u)}{J_1^2(u)}\right] \quad (15)$$

where r_s is the spot size radius and P is the optical power carried by the $\rm HE_{11}$ mode. β is the propagation constant in the z direction, and v is the normalized frequency. u and w are the normalized transverse wavenumbers in the r direction in the core and cladding, respectively. J_m is the mth-order Bessel function.

The r_s value is known to be related to both the v value and the radius a of the core layer as follows [35]:

$$r_s = a\left(0.65 + \frac{1.619}{v^{\frac{3}{2}}} + \frac{2.879}{v^6}\right). \quad (16)$$

In the following subsection, we frequently use the average power density $I_{\rm AV}$ defined by the following equation:

$$I_{\rm AV} = \frac{P}{\pi r_s^2}. \quad (17)$$

B. Several Conditions for Heat Conduction

Silica glass has a melting point of 1996 K at which it changes from the amorphous solid phase to the viscous liquid phase [36]. The phase transition of the silica glass causes the temperature dependence of the specific heat C_p to change drastically. The $C_p(T)$ values (kJ $\cdot$ kg^{-1} $\cdot$ K^{-1} unit) of the silica glass are given by [36]

$$C_p = \begin{cases} 1.195 + 3.154 \times 10^{-5}T \\ \quad -6.514 \times 10^4 T^{-2}, & \text{if } T \le 1996 \text{ K} \\ 1.430, & \text{if } T > 1996 \text{ K}. \end{cases} \quad (18)$$

Furthermore, the silica glass has a vaporization (or thermal decomposition) point of about 3000 K, where it changes from

TABLE I
THERMAL PROPERTIES OF SILICA GLASS IN VARIOUS PHASES

Phase	ρ (kg m^{-3})	κ (W m^{-1} K^{-1})
Solid	2200	9.2
Liquid	2200	9.2
Vapor	1530	0.03

the liquid phase to the vapor phase [36]. At $T >\sim 3000$ K, substantially all of the silica glass is thermally decomposed to the mixture of SiO and O_2 gas, as shown in Fig. 3. High-density O_2 gas [7], [37] is produced in this vaporization process. Therefore, it is assumed that the C_p value in the vapor phase is the same as that (1.323 kJ kg^{-1}K^{-1}) of the high-density O_2 gas.

The thermal properties (ρ and κ values) of the silica glass are summarized in Table I.

We solved (13) by using the explicit finite-difference method (FDM) [38] under the boundary and initial conditions described below. The area for the numerical calculation had a length $2L$ ($=$ 4 cm) in the axial (z) direction and a width $2r_f$ ($= 125$ μm) in the radial (r) direction. There were 24 and 2000 divisions in $2r_f$ and $2L$, respectively, and we set the calculation time interval at 1 μs. We assumed that the hot zone was located at the center of the fiber (length $2L$) and that the length ΔL of the hot zone was 500 μm.

The boundary conditions are as follows.

1) There is an axisymmetrical T distribution of the optical fiber, whose center axis is located at $r = 0$.
2) There is a heat source $\dot{Q}$ given by (14) at the hot zone in the fiber core.
3) Heat loss is assumed to occur through radiation from the surfaces of the fiber cladding and the fiber ends ($z = \pm L$) as follows:

$$-\kappa \frac{\partial T}{\partial r}\bigg|_{r=r_f} = \sigma_s \epsilon_e \left(T^4 - T_a^4\right) \tag{19}$$

$$-\kappa \frac{\partial T}{\partial z}\bigg|_{z=\pm L} = \sigma_s \epsilon_e \left(T^4 - T_a^4\right) \tag{20}$$

where σ_s is the Stefan–Boltzmann constant and $\epsilon_e (\sim 0.9)$ is the emissivity of the surface. Below, T_a is assumed to be 298 K.

By contrast, the initial conditions are that the T value of the optical fiber, except in the hot zone, is T_a at $t = 0$ and that the core-center temperature T_c in the hot zone equals T_c^0.

When the core layer is heated above the vaporization point of silica (~ 3000 °C), an enclosed hollow cavity is produced in the core center. This cavity contains oxygen, which is produced by the reaction given by (6). The heat conductivity κ of the oxygen (0.03 W·m^{-1}·K^{-1}) is two orders smaller than that of the silicate glass. Therefore, the heat transferred in the silica core will be stopped at the cavity. We assume that the cavity has a refractive index $n_v \sim 1$ and a length l_c.

When the light propagates through the fiber core along the z direction (the direction away from the light source), the P value decreases because of the light absorption α. The light propagating in the core layer will be reflected at the cavity wall. When the light direction is reversed at the cavity, the multiple reflection in the cavity walls must be considered. In this case the light propagates through the fiber core of length $L - \Delta z$, and then back and forth in the hot zone, whose length and absorption are Δz and α_h, respectively. By considering these points, the P value is given by

$$P = P_0 R_f \exp\left(-2\alpha_h \Delta z - \int_{-L}^{-\Delta z} \alpha(T) dz\right) \tag{21}$$

where P_0 is the initial optical power and R_f is the reflectance of the optical power at the cavity. The R_f values under multiple reflection are given by [39]

$$R_f = \frac{4R \sin^2\left(\frac{2\pi l_c}{\lambda}\right)}{(1-R)^2 + 4R \sin^2\left(\frac{2\pi l_c}{\lambda}\right)} \tag{22}$$

where λ is the wavelength of the guided light in the SM fiber and R is the reflectivity at the boundary of the silica core and the cavity. R is given by

$$R = \left(\frac{n_1 - 1}{n_1 + 1}\right)^2. \tag{23}$$

As shown in (22), the R_f value under multiple reflection depends on the cavity length l_c.

In the following section, we describe the calculated time (t) dependence of $T(r, z)$ in SM optical fibers.

C. Propagation of Fiber Fuse in SM Optical Fiber

In the calculation, we used the refractive index data of $n_1 = 1.4617$ and $n_0 = 1.4573$ at $\lambda = 1.064$ μm, where n_0 is the refractive index of the cladding. In this case, the v value was about 3.34, and the spot size radius r_s was about 4.5 μm.

We calculated the $T(r, z)$ values at $t = 6$, 22, and 38 ms when $T_c^0 = 2723$ K and $P_0 = 2$ W. The calculated results are shown in Figs. 6–8. As shown in Fig. 6, the core-center temperature near the hot-zone end ($z \sim 0$ mm) changes abruptly to the large value of $> 3.5 \times 10^5$ K after 6 ms. This rapid heating phenomenon initiates the "fiber fuse" phenomenon as shown in Figs. 7 and 8. We define this time (6 ms) as the beginning time t_b of a fiber fuse. After 22 and 38 ms, the high-temperature front in the core layer reached -6.6 and -13.8 mm, respectively. The average propagation velocity v_f can be estimated to be 0.42 m s^{-1} by using these data.

Next we investigated the P_0 dependence of both the t_b and v_f values. There was no fiber fuse when $P_0 < 0.98$ W. We estimated the t_b and v_f values from the time course of the fiber-fuse front positions in the core layer at various P_0 values from 0.98 to 10 W when $T_c^0 = 2723$ K. The calculated results are shown in Fig. 9. It is clear that the t_b value increases as the P_0 value decreases, and there is a rapid increase in the t_b value below $P_0 < 0.98$ W. We define this P_0 value (0.98 W) as the threshold power $P_{\rm th}$ at 1.064 μm for the beginning of the fiber fuse.

The v_f value increases as the P_0 value increases. It is well known that there is a linear relationship between the v_f values and the average power density $I_{\rm AV}$, rather than the P_0 value [7], [12]–[14]. Fig. 10 shows the $I_{\rm AV}$ dependence of the v_f value. The data reported by Kashyap for Fiber A [7] and those reported by Davis *et al.* for SMF28 fiber [12] are plotted in this figure. When we plotted the data obtained by Kashyap [7], we used

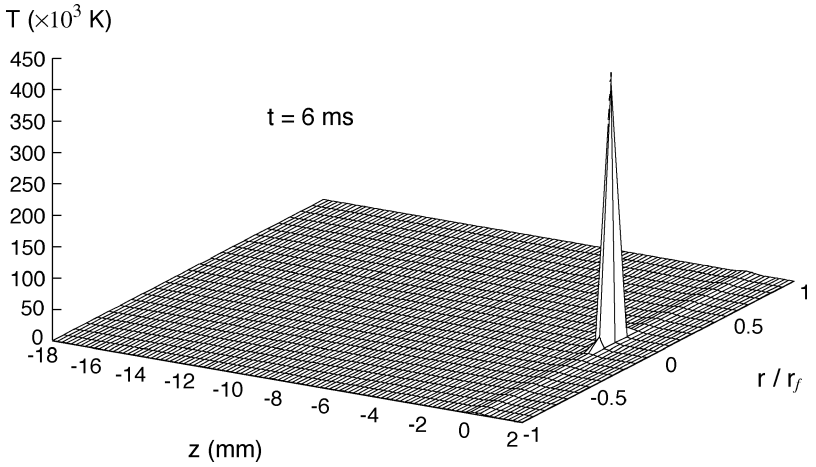

Fig. 6. Temperature field in SM optical fiber after 6 ms when $P_0 = 2$ W and $T_c^0 = 2723$ K.

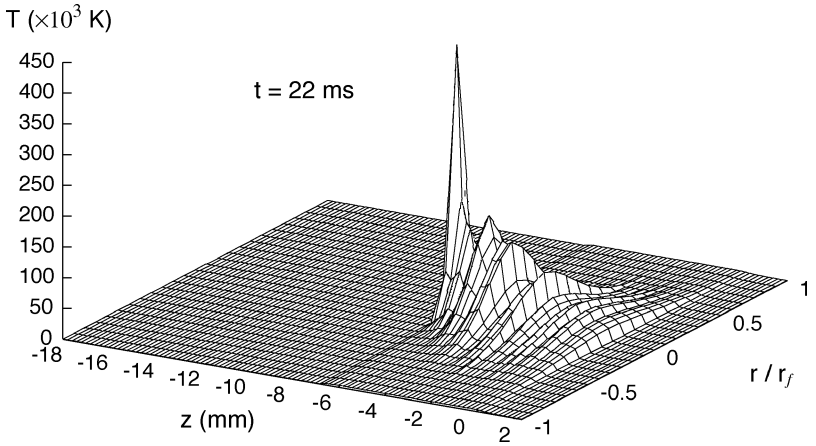

Fig. 7. Temperature field in SM optical fiber after 22 ms when $P_0 = 2$ W and $T_c^0 = 2723$ K.

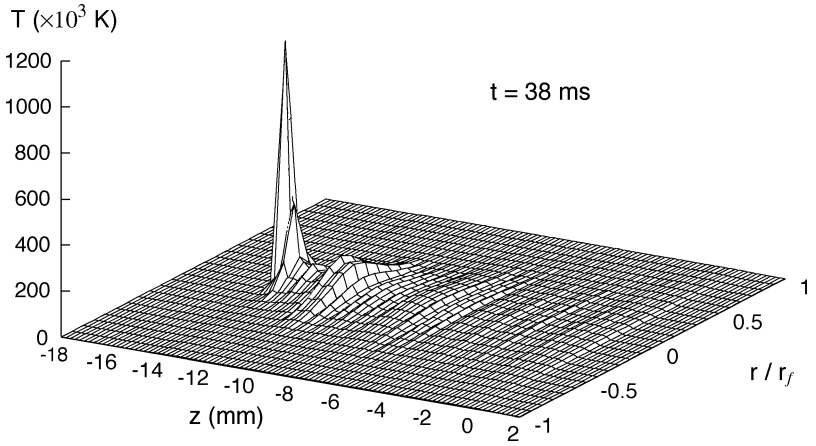

Fig. 8. Temperature field in SM optical fiber after 38 ms when $P_0 = 2$ W and $T_c^0 = 2723$ K.

$r_s = 3.82$ μm, which was estimated by using $v \sim 3.11$, $a = 4.03$ μm, and (16). As shown in Fig. 10, the v_f value is linearly proportional to the $I_{\rm AV}$ value. The calculated v_f values agree well with the experimental values.

By contrast, Dianov *et al.* reported that the experimentally determined threshold intensity $I_{\rm th}(\equiv P_{\rm th}/\pi r_s^2)$ was about 1.45 MW $\cdot$ cm^{-2} at 1.064 μm when $r_s = 4.5$ μm [5]. As shown in Fig. 10, the theoretical $I_{\rm th}$ value is about 1.54 MW$\cdot$cm^{-2}, which is almost the same as the experimental value (1.45 MW $\cdot$ cm^{-2}).

D. Wavelength Dependence of Threshold Power

It is well known that a pump source with a high optical power is needed to obtain a large Raman gain in Raman amplifier-based optical network systems [2], [4]. The $P_{\rm th}$ value, therefore,

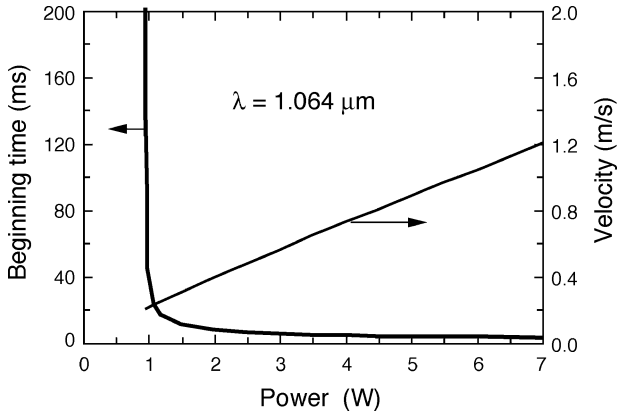

Fig. 9. Power dependence of the beginning time and the propagation velocity when $T_c^0 = 2723$ K.

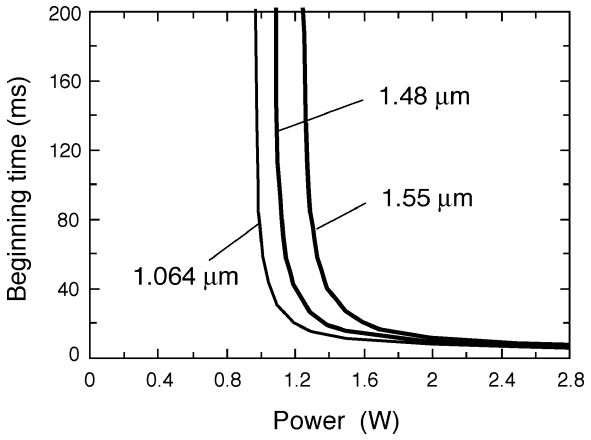

Fig. 11. Power dependence of the beginning times at 1.064, 1.48, and 1.55 μm.

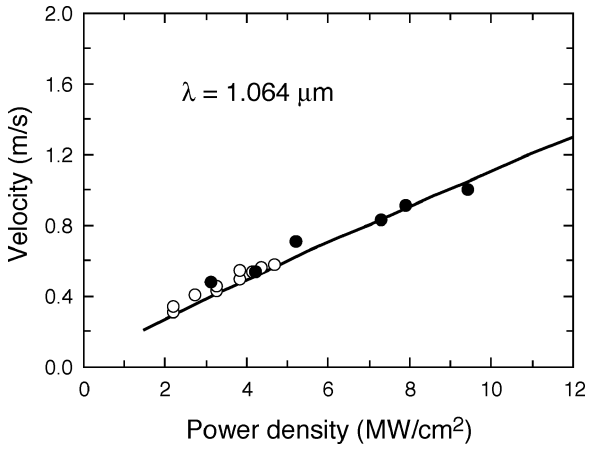

Fig. 10. Power density dependence of the propagation velocity when $T_c^0 = 2723$ K. The open circles are the data reported by Kashyap [7] and the closed circles are the data reported by Davis *et al.* [10].

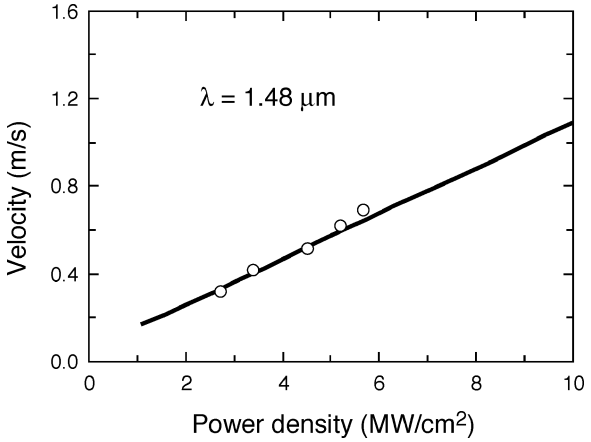

Fig. 12. Power density dependence of the propagation velocity at 1.48 μm. The open circles are the data reported by Atkins *et al.* [15].

becomes a measure of the upper safety limits of both the pump and the Raman amplified optical power. We estimated the $P_{\rm th}$ values, and the $I_{\rm AV}$ dependence of the v_f values at two wavelengths, 1.48 and 1.55 μm. The former (1.48 μm) is the typical wavelength of the pump laser for Raman amplifiers, and the latter (1.55 μm) is the typical wavelength used for optical-fiber communications.

In the calculation, we used refractive index data of $n_1 = 1.4569$ and $n_0 = 1.4525$ at 1.48 μm and $n_1 = 1.4560$ and $n_0 = 1.4517$ at 1.55 μm. In this case, the v values at 1.48 and 1.55 μm were about 2.40 and 2.29, respectively. The r_s values at 1.48 and 1.55 μm, which were estimated by using the v values, $a = 5$ μm, and (16), were about 5.5 and 5.7 μm, respectively. The hot zone temperature T_c^0 was set at 2773 K at 1.48 and 1.55 μm, which was 50 K higher than that for $\lambda = 1.064$ μm.

We calculated the P_0 dependence of the t_b values at 1.48 and 1.55 μm. The calculated results are shown in Fig. 11, together with the results for $\lambda = 1.064$ μm. From this figure, we can estimate the $P_{\rm th}$ values at 1.064, 1.48, and 1.55 μm to be 0.98, 1.10, and 1.26 W, respectively. It is clear that the $P_{\rm th}$ value increases as the laser wavelength increases. A similar phenomenon was reported by Seo *et al.* [40].

By contrast, Dianov *et al.* reported that the experimentally determined $I_{\rm th}$ values were almost constant (~ 1 MW $\cdot$ cm^{-2}) when the r_s values were larger than ~ 5 μm [5]. Therefore, we estimated the $I_{\rm th}$ values by using the $P_{\rm th}$ and r_s values at 1.48 and 1.55 μm. The calculated $I_{\rm th}$ values were about 1.16 MW $\cdot$ cm^{-2} at 1.48 μm ($r_s = 5.5$ μm) and about 1.23 MW $\cdot$ cm^{-2} at 1.55 μm ($r_s = 5.7$ μm). These theoretical $I_{\rm th}$ values agree well with the experimental value (~ 1 MW $\cdot$ cm^{-2}).

Next, we examined the $I_{\rm AV}$ dependence of the v_f values at 1.48 and 1.55 μm. Fig. 12 shows the $I_{\rm AV}$ dependence of the v_f value at 1.48 μm. The data reported by Atkins *et al.* [15] are plotted in this figure. The calculated v_f values agree well with the experimental values. The v_f value is linearly proportional to the $I_{\rm AV}$ value, and the slope of the line is similar to that shown in Fig. 10. To clarify this, the $I_{\rm AV}$ dependence of the v_f values at 1.064, 1.48, and 1.55 μm are plotted in Fig. 13. It is clear that the relation curve between the $I_{\rm AV}$ and the v_f value of 1.064 μm is almost the same as the curve of 1.48 μm. However, the v_f values estimated at 1.55 μm were smaller than those of 1.064 and/or 1.48 μm. It is not clear why this phenomenon occurs only at 1.55 μm and is not observed at 1.48 μm. If we are to clarify this phenomenon, we must undertake experimental studies of the v_f measurements at 1.55 μm. Further investigations focused on the

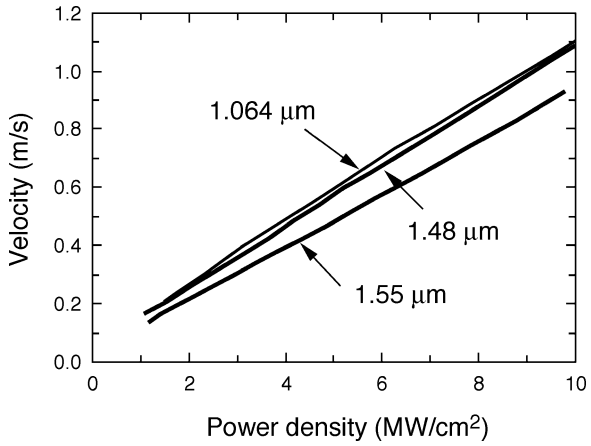

Fig. 13. Power density dependence of the propagation velocities at 1.064, 1.48, and 1.55 μm.

fiber fuse phenomena at 1.48 and 1.55 μm are under way in our laboratories.

IV. Conclusion

The large absorption coefficient α of SM optical fiber at high temperatures is closely related to the generation of the fiber fuse phenomenon. We considered a high-temperature loss-increase mechanism, which includes two factors that bring about an increase in the α values: 1) electronic conductivity caused by the thermal ionization of a Ge-doped silica core and 2) thermochemical SiO production in silica glass. By using the mechanism, we estimated the α values of Ge-doped silica-core fibers at high temperatures. Then we studied the unsteady-state thermal conduction process in a step-index SM fiber theoretically using the explicit finite-difference method. The core-center temperature changed suddenly and reached over 4×10^5 K when a 1.064-μm laser power of 2 W was input into the core layer heated at 2723 K. This rapid heating of the core initiated the "fiber fuse" phenomenon. The high-temperature core areas were enlarged and propagated toward the light source. The propagation rates of the fiber fuse estimated at 1.064 and 1.48 μm were in fair agreement with the experimentally determined values. We found that the threshold power for the beginning of the fiber fuse increases from 0.98 to 1.26 W when the input laser wavelength is increased from 1.06 to 1.55 μm.

Acknowledgment

The authors would like to thank Dr. H. Toba and Dr. M. Koga for their advice and encouragement.

References

[1] Y. Aoki, "Fiber Raman amplifier properties for applications to long-distance optical communications," *Opt. Quantum Electron.*, vol. 21, pp. S89–S104, 1989.

[2] P. B. Hansen, L. Eskildsen, S. G. Grubb, A. J. Stentz, T. A. Strasser, J. Judkins, J. J. DeMarco, R. Pedrazzani, and D. J. DiGiovanni, "Capacity upgrades of transmission systems by Raman amplification," *IEEE Photon. Technol. Lett.*, vol. 9, pp. 262–264, Feb. 1997.

[3] H. Suzuki, J. Kani, H. Masuda, N. Tachio, K. Iwatsuki, Y. Tada, and M. Sumida, "1-Tb/s (100 × 10 Gb/s) super-dense WDM transmission with 25-GHz channel spacing in the zero-dispersion region employing distributed Raman amplification technology," *IEEE Photon. Technol. Lett.*, vol. 12, pp. 903–905, July 2000.

[4] S. Namiki and Y. Emori, "Ultrabroad-band Raman amplifiers pumped and gain-equalized by wavelength-division-multiplexed high-power laser diodes," *IEEE J. Select. Topics Quantum Electron.*, vol. 7, pp. 3–16, Jan./Feb. 2001.

[5] E. M. Dianov, I. A. Bufetov, A. A. Frolov, V. G. Plotnichenko, V. M. Mashinskii, M. F. Churbanov, and G. E. Snopatin, "Catastrophic destruction of optical fibers of various composition caused by laser radiation," *Quantum Electron.*, vol. 32, no. 6, pp. 476–478, 2002.

[6] R. Kashyap and K. J. Blow, "Observation of catastrophic self-propelled self-focusing in optical fibers," *Electron. Lett.*, vol. 24, no. 1, pp. 47–49, 1988.

[7] R. Kashyap, "Self-propelled self-focusing damage in optical fibers," in *Proc. Int. Conf. Lasers*, Dec. 1988, pp. 859–866.

[8] T. J. Driscoll, J. M. Calo, and N. M. Lawandy, "Explaining the optical fuse," *Opt. Lett.*, vol. 16, pp. 1046–1048, July 1991.

[9] D. P. Hand and P. S. J. Russell, "Solitary thermal shock waves and optical damage in optical fibers: the fiber fuse," *Opt. Lett.*, vol. 13, no. 9, pp. 767–769, 1988.

[10] ——, "Soliton-like thermal shock-waves in optical fibers: origin of periodic damage tracks," in *Proc. Eur. Conf. Opt. Commun.*, Sept. 1988, pp. 111–114.

[11] D. D. Davis, S. C. Mettler, and D. J. DiGiovanni, "Experimental data on the fiber fuse," *Proc. SPIE*, vol. 2714, pp. 202–210, June 1995.

[12] ——, "A comparative evaluation of fiber fuse models," *Proc. SPIE*, vol. 2966, pp. 592–606, June 1996.

[13] R. Kashyap, A. Sayles, and G. F. Cornwell, "Heat flow modeling and visualization of catastrophic self-propagating damage in singlemode optical fibers at low powers," *Proc. SPIE*, vol. 2966, pp. 586–591, June 1996.

[14] R. Kashyap, "High average power effects in optical fibers and devices," *Proc. SPIE*, vol. 4940, pp. 108–117, June 2003.

[15] R. M. Atkins, P. G. Simpkins, and A. D. Yabon, "Track of a fiber fuse: a Rayleigh instability in optical waveguides," *Opt. Lett.*, vol. 28, no. 12, pp. 974–976, 2003.

[16] A. E. Owen and R. W. Douglas, "The electrical properties of vitreous silica," *J. Soc. Glass Technol.*, vol. 43, pp. 159–178, June 1959.

[17] R. H. Doremus, "Ionic transport in amorphous oxides," *J. Electrochem. Soc.*, vol. 115, pp. 181–186, Feb. 1968.

[18] Y. Hibino and H. Hanafusa, "ESR study on E'-centers induced by optical fiber drawing process," *Jpn. J. Appl. Phys.*, vol. 22, no. 12, pp. L766–L768, 1983.

[19] H. Hanafusa, Y. Hibino, and F. Yamamoto, "Formation mechanism of drawing-induced E' centers in silica optical fibers," *J. Appl. Phys.*, vol. 58, no. 3, pp. 1356–1361, 1985.

[20] E. J. Friebele, D. L. Griscom, and G. H. Sigel Jr, "Defect centers in a germanium-doped silica-core optical fiber," *J. Appl. Phys.*, vol. 45, no. 8, pp. 3424–3428, 1984.

[21] A. M. Goodman, "Electron Hall effect in silicon dioxide," *Phys. Rev.*, vol. 164, no. 3, pp. 1145–1150, 1967.

[22] Y. Shuto, S. Yanagi, S. Asakawa, M. Kobayashi, and R. Nagase, "Simulation of fiber fuse phenomenon in single-mode optical fibers," *J. Lightwave Technol.*, vol. 21, pp. 2511–2517, Nov. 2003.

[23] A. N. Gur'yanov, D. D. Gusovskii, E. M. Dianov, L. S. Kornienko, E. P. Nikitin, A. O. Rybaltovskii, V. F. Khopin, P. V. Chernov, and A. S. Yushin, "Radiation-optical stability of low-loss glass-fiber waveguides," *Sov. J. Quantum Electron.*, vol. 9, no. 6, pp. 768–773, 1979.

[24] E. J. Friebele and M. E. Gingerich, "Radiation-induced optical absorption bands in low loss optical fiber waveguides," *J. Non-Cryst. Solids*, vol. 38&39, pp. 245–250, 1980.

[25] R. C. Hughes, "Charge-carrier transport phenomena in amorphous SiO_2: direct measurement of drift mobility and lifetime," *Phys. Rev. Lett.*, vol. 30, no. 26, pp. 1333–1336, 1973.

[26] H. L. Schick, "A thermodynamic analysis of the high-temperature vaporization properties of silica," *Chem. Rev.*, vol. 60, pp. 331–362, 1960.

[27] L. Brewer and R. K. Edwards, "The stability of SiO solid and gas," *J. Phys. Chem.*, vol. 58, pp. 351–358, 1954.

[28] *JANAF Thermochemical Tables*, U.S. Department of Commerce and National Bureau of Standards, 2nd ed., 1971.

[29] H. R. Philipp, "Optical properties of noncrystalline Si, SiO, SiO_x and SiO_2," *J. Phys. Chem. Solids*, vol. 32, pp. 1935–1945, 1971.

[30] ——, "Optical and bonding model for noncrystalline SiO_x and SiO_xN_y materials," *J. Non-Cryst. Solids*, vol. 8–10, pp. 627–632, 1972.

[31] W. C. Dash and R. Newman, "Intrinsic optical absorption in single-crystal germanium and silicon at 77°K and 300°K," *Phys. Rev.*, vol. 99, no. 4, pp. 1151–1155, 1955.
[32] G. G. Macfarlane, T. P. McLean, J. E. Quarrington, and V. Roberts, "Fine structure in the absorption-edge spectrum of Si," *Phys. Rev.*, vol. 111, no. 5, pp. 1245–1254, 1958.
[33] G. G. Macfarlane and V. Roberts, "Infrared absorption of silicon near the lattice edge," *Phys. Rev.*, vol. 98, no. 6, pp. 1865–1866, 1955.
[34] H. S. Carslaw and J. C. Jaeger, *Conduction of Heat in Solids*, 2nd ed. Oxford, U.K.: Oxford Univ. Press, 1959, ch. 13.
[35] D. Marcuse, "Loss analysis of single-mode fiber splices," *Bell Syst. Tech. J.*, vol. 56, no. 5, pp. 703–718, 1977.
[36] I. Barin and O. Knacke, *Thermochemical Properties of Inorganic Substances*. Berlin, Germany: Springer-Verlag, 1973, p. 690.
[37] E. M. Dianov, V. M. Mashinsky, V. A. Myzina, Y. S. Sidorin, A. M. Streltsov, and A. V. Chickolini, "Change of refractive index profile in the process of laser-induced fiber damage," *Sov. J. Lightwave Commun.*, vol. 2, pp. 293–299, 1992.
[38] G. E. Forsythe and W. R. Wasow, *Finite-Difference Methods for Partial Differential Equations*. New York: Wiley, 1960, ch. 2.
[39] M. Born and E. Wolf, *Principles of Optics*, 7th ed. Cambridge, U.K.: Cambridge Univ. Press, 2001, ch. 7.
[40] K. Seo, N. Nishimura, M. Shiino, R. Yuguchi, and H. Sasaki, "Examination of threshold power for high-power problems in optical fiber," in *Proc. Int. Laser Safety Conf.*, Mar. 2003, pp. 298–302.

Yoshito Shuto (M'90) received the B.S., M.S., and Ph.D. degrees from Kyushu University, Fukuoka, Japan, in 1977, 1979, and 1990, respectively.

He joined Nippon Telegraph and Telephone Corporation (NTT), Ibaraki, Japan, in 1979, where he was involved in research on oriented crystalline and liquid-crystalline polymer materials for optical-fiber jackets and diazo-dye-substituted polymer materials for second-order nonlinear optics. He is presently engaged in research on injection molding polymer materials for optical connection technology with NTT Photonics Laboratories.

Dr. Shuto is a member of the Institute of Electronics, Information and Communication Engineers, the Japan Society of Applied Physics, the Optical Society of Japan, and the Optical Society of America.

Shuichi Yanagi received the B.S., M.S., and Ph.D. degrees from Keio University, Yokohama, Japan, in 1992, 1994, and 1997, respectively.

In 1997 he joined the NTT Opto-electronics Laboratories, Ibaraki, Japan. He is presently engaged in research on injection molding polymer materials for optical connection technology with NTT Photonics Laboratories.

Dr. Yanagi is a member of the Institute of Electronics, Information and Communication Engineers and the Japan Society of Applied Physics.

Shuichiro Asakawa (M'96) received the B.E., M.E., and D.E. degrees in electrical and computer engineering from Yokohama National University, Yokohama, Japan, in 1990, 1992, and 1995, respectively.

He joined the NTT Photonics Laboratories, Atsugi, Japan, in 1995. He has been engaged in research on optical connectors.

Dr. Asakawa is a member of the Institute of Electronics, Information and Communication Engineers.

Masaru Kobayashi (M'96) received the B.E., M.E., and D.E. degrees in mechanical engineering from Nagoya University, Nagoya, Japan, in 1986, 1988, and 2004, respectively.

He joined the NTT Photonics Laboratories, Atsugi, Japan, in 1988, where he has been involved in research on high-resolution optical reflectometry for characterizing optical waveguide components, and in development of optical fiber connectors.

Dr. Kobayashi is a member of the Institute of Electronics, Information and Communication Engineers and the Japan Society of Applied Physics.

Ryo Nagase (M'90) received the B.E., M.E., and Ph.D. degrees in precision engineering from Tohoku University, Miyagi, Japan, in 1983, 1985, and 1998, respectively.

He joined the NTT Photonics Laboratories, Atsugi, Japan, in 1985, where he has been invovled in the research and development of optical fiber connectors. From 1992 to 1994, his fields of interest were photonic switching systems. Since 1994, he has been involved in the research of optical components for fiber-optic communication systems, passive components such as optical fiber cables, and planar lightwave circuits. He is presently a manager in the research and development of optical fiber connection technology.

Dr. Nagase is a member of the Institute of Electronics, Information and Communication Engineers and the Japan Society of Mechanical Engineers.